Synchrotron excitation, emission and theoretical simulation of lanthanide ions in hexachloroelpasolite crystals

2009 J. Phys.: Condens. Matter 21 395501

(http://iopscience.iop.org/0953-8984/21/39/395501)

J. Phys.: Condens. Matter **21** (2009) 395501 (8pp) doi:10.1088/0953-8984/21/39/395501

Synchrotron excitation, emission and theoretical simulation of lanthanide ions in hexachloroelpasolite crystals

Chang-Kui Duan[1,2], Peter A Tanner[2], Andries Meijerink[3] and Vladimir Babin[3]

[1] Institute of Modern Physics, Chongqing University of Post and Telecommunications, Chongqing 400065, People's Republic of China
[2] Department of Biology and Chemistry, City University of Hong Kong, Tat Chee Avenue, Kowloon, Hong Kong SAR, People's Republic of China
[3] Debye Institute, Department of Chemistry, Utrecht University, Princetonplein 5, 3584 CC Utrecht, The Netherlands

Received 13 July 2009, in final form 6 August 2009
Published 1 September 2009
Online at stacks.iop.org/JPhysCM/21/395501

Abstract
Emission and excitation spectra of $Cs_2NaLnCl_6$ (Ln = Y, Eu, Gd, Er, Yb), Cs_2NaYCl_6:Ce and Cs_2NaYCl_6:Tm have been recorded using synchrotron radiation. With the possible exception of the case for Ce^{3+}, no 5d → 4f transitions are observed and the emission spectra are entirely assigned to 4f → 4f intraconfigurational transitions of Ln^{3+} in $LnCl_6^{3-}$ and impurity species. The excitation spectra comprise intraconfigurational, charge transfer and band-to-band transitions. Trace impurities of oxy-species or of other lanthanide ions have a profound effect upon the spectra. The 4f–5d absorption spectra have been simulated by employing the suite of programs of Professor M F Reid and the results have been included together with the experimental spectra.

(Some figures in this article are in colour only in the electronic version)

1. Introduction

The absorption and luminescence spectra of lanthanide hexachloroelpasolites $Cs_2NaLnCl_6$ have been extensively studied and were reviewed in 2004 [1]. These studies have concerned the intraconfigurational $4f^N - 4f^N$ transitions of Ln^{3+}, and the $Fm3m$ cubic symmetry of the host lattice not only confers high degeneracies to the crystal-field energy levels but also introduces strict selection rules for the electronic transitions. By contrast, although the interconfigurational $4f^N - 4f^{N-1}5d$ transitions of $Cs_2NaLnCl_6$ are electric dipole allowed (subject to the site symmetry selection rules), because the spectral features are located at higher energies there have been few investigations. This is also because the band gaps of these systems are relatively low (7.4 ± 0.8 eV) and the systems are deliquescent. Some previous studies are available for the electronic absorption spectra $Cs_2NaLnCl_6$ with Ln = Ce [2], Pr [3], Tb [4], and the excited state absorption of Nd^{3+} [5]. The first report of the $4f^N - 4f^{N-1}5d$ absorption transitions for several '$LnCl_6^{3-}$' systems was the solution study by Ryan and Jørgensen [6]. Subsequently, calculations were presented for the lowest $4f^N - 4f^{N-1}5d$ and charge transfer (CT) energies of $LnCl_6^{3-}$ complexes by Ionova *et al* [7]. These investigations have been extended both experimentally and theoretically in the present study through the preliminary investigation of the emission and excitation spectra of $Cs_2NaLnCl_6$ (Ln = Y, Eu, Gd, Er, Yb), Cs_2NaYCl_6:Ce and Cs_2NaYCl_6:Tm, using synchrotron radiation. It is observed that the $4f^N - 4f^{N-1}5d$ transition energies lie above the host band gaps for most of the series, by contrast to the case for wide band gap fluoride systems [8–11].

2. Experimental section

The neat hexachloroelpasolite crystals were synthesized by the Bridgman method [2] in sealed quartz tubes from Ln_2O_3 (Strem Chemicals, 99.99% purity). Stoichiometric quantities of NaCl and CsCl were added to a solution of Ln_2O_3 in concentrated HCl and the mixture was carefully taken to dryness. The resulting powder was rapidly transferred to a heated quartz tube and pumped under vacuum at 450 °C for

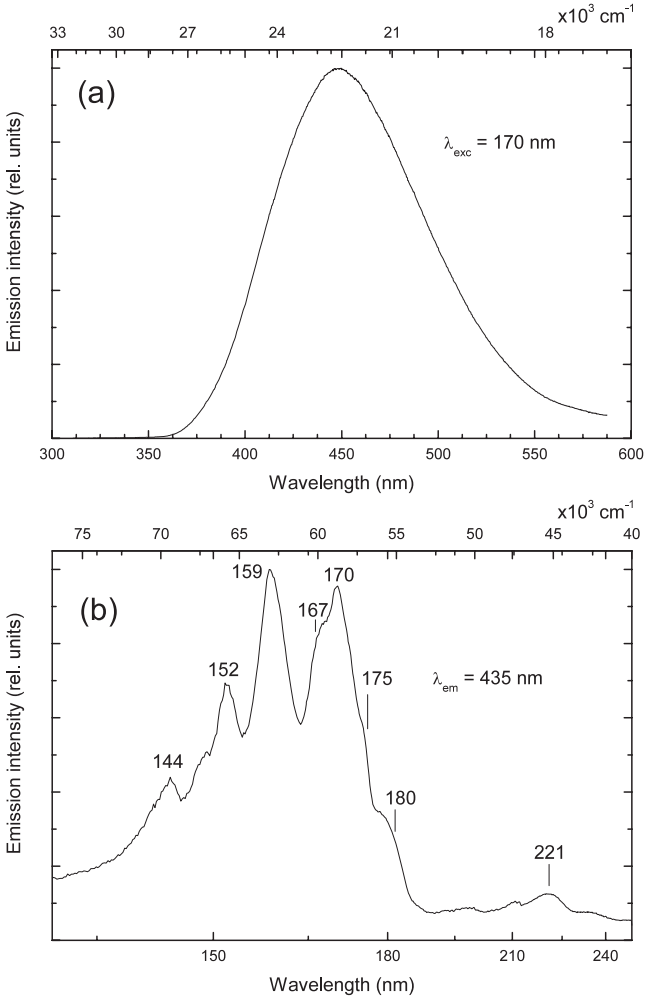

Figure 1. Cs_2NaYCl_6. (a) 11 K emission spectrum between 330 and 585 nm. (b) Excitation spectrum between 130 and 250 nm.

two days. Then the tube was sealed and passed through the furnace at 850 °C. The diluted systems Cs_2NaYCl_6:Ce and Cs_2NaYCl_6:Tm were prepared analogously. The ampoules were broken just before mounting the crystals. Luminescence and excitation spectra were recorded on crystals of 1–2 mm thickness at 10 K at the HIGITI UV/VUV beamline at the DESY synchrotron in Hamburg, Germany, with detection using a solar blind photomultiplier or a charge coupled device. The slit width was set so that a resolution of 2.5 nm was obtained for the excitation spectra. The experimental methods have been described previously [12].

Since the hexachloroelpasolites are extremely sensitive to moisture, various impurity bands were observed in our spectra. In the case of neat Cs_2NaYCl_6, under 170 nm excitation at 11 K, a broad band extending from 360 to 580 nm (FWHM 93 nm) was observed, with maximum intensity at 448 nm (22 285 cm^{-1}) (figure 1(a)). This band corresponds either to an impurity or to self-trapped exciton emission. The excitation spectrum obtained by monitoring at 435 nm (figure 1(b)) shows a weak band at 45 152 cm^{-1} (221 nm), with major peaks in order of decreasing intensity at 58 747, 63 089, 65 917 and 69 394 cm^{-1}. The first of these strong bands (at 170 nm) has shoulders to longer wavelength at 57 082, 55 433 cm^{-1} (175, 180 nm).

Table 1. The parameter values (cm^{-1}) used in the simulation of $4f^N - 4f^{N-1}5d$ absorption spectra. Refer to the text for the explanation.

Ions	Eu^{3+}	Gd^{3+}	Er^{3+}	Tm^{3+}	Yb^{3+}
F^2	83 902	78 686	96 717	99 725	106 963
F^4	59 990	70 120	67 374	68 592	73 841
F^6	41 364	43 596	47 541	48 231	51 997
ζ_{4f}	1324	1505	2363	2616	2898
α	17	37	18	19	
β	−640	−1905	−655	−730	
γ	1750	1679	2500	2716	
M^0	2.4	1.6	4.1	3.8	
P^2	245	0	510	43	
T^2	370	0	120	120	
T^3	40	0	50	50	
T^4	40	0	56	56	
T^6	−330	0	−286	−286	
T^7	380	0	191	191	
T^8	370	0	176	176	
B_4(f)	1928	1776	1555	1787	1454
B_6(f)	247	139	154	170	79
E_{exc}	64 300	67 440	82 650	84 700	89 200
B_4(d)	37 126	36 809	35 543	35 200	34 900
η_{fd}	0.53	0.53	0.53	0.53	0.53
ζ_{5d}	1080	1132	1346	1400	1453

3. Theory

The detailed method of simulation of the $4f^{N-1}5d$ energy levels and spectral intensities of $4f^N \rightarrow 4f^{N-1}5d$ transitions has been previously described for the series Cs_2NaYF_6:Ln^{3+} [9] and only a brief description of the parameters in the Hamiltonian [13] is given here. The $4f^N$ and $4f^{N-1}5d$ multi-electron energy levels were calculated using the standard phenomenological crystal-field Hamiltonian H(4f) and its extension [9]:

$$H = H(4f) + H(5d) + H_{int}(4f, 5d), \quad (1)$$

where H(4f), H(5d) and H_{int}(4f, 5d) describe the interactions experienced by, or between, the 4f electrons; those experienced by the 5d electron; and the interaction between 4f and 5d electrons, respectively. For H(4f), E_{avg} is a parameter for shifting all the levels so that the energy of the lowest level of $4f^N$ is zero; the second and third terms in H(4f) are the two strongest interactions for the $4f^N$ configuration ($4f^{N-1}$ core), i.e., parameterized by the Coulomb (F^k (k = 2, 4, 6)) and spin–orbit (ζ_{4f}) interactions; the last term in H(4f) is the crystal-field interaction felt by 4f electrons, with the parameters B_4(f) and B_6(f); and the other terms are effective interactions used to describe various effects due to configuration interaction. The α, β and γ parameters are associated with two-electron correlation corrections to the Coulomb repulsion. The T^i are parameters for three-electron correlation. The usual choice of $M^2 = 0.56M^0$, $M^4 = 0.31M^0$, $P^4 = 0.5P^2$, and $P^6 = 0.1P^2$ has been adopted and those parameters are not given explicitly in table 1. For

Table 2. The onset of 4f–5d absorption (E_{4f-5d}); Cl^-–Ln^{3+} CT energy (E_{CT}); and the excitation band maximum at ∼10 K in the region of the excitonic near-band-edge transition (CB) for lanthanide hexachloroelpasolites. All values are in units of 10^3 cm^{-1}.

Ln^{3+}	ΔE_{4f-5d}[a]	E_{4f-5d}(calc)[b]	ΔE_{CT}[c]	E_{CT}(calc)[d]	E_{CT}(exp)[e]	CB[e]
Eu^{3+}	35.9	64.1	0	37.5[e]	37.5	52.6
Gd^{3+}	45.8	74.0				54.6
Er^{3+}	30.0 (26.95)	58.2 (55.15)	18.9	56.4	56.5	52.9
Tm^{3+}	29.0 (26.95)	57.2 (55.15)	14.3	51.8	48.1	52.1
Yb^{3+}	38.0	66.2	3.8	41.3		

[a] From [20]; relative to Ce^{3+}.
[b] From equation (1). Values in parentheses refer to spin-forbidden transitions.
[c] From [21]; relative to Eu^{3+}.
[d] From equation (2).
[e] This work.

H(5d), the two terms include parameters for the spin–orbit (ζ_{5d}) and the strong crystal-field interactions (B_4(d)) felt by the 5d electron. For the H_{int}(4f, 5d) interaction, E_{exc} describes the separation between the barycenters of the $4f^N$ and $4f^{N-1}5d$ levels; and there are parameters for the direct F^k(fd) and for the exchange G^k(fd) Coulomb interaction between 4f and 5d electrons.

The parameters and their values used in the present calculations are listed in table 1. These parameters were not fitted, except for E_{exc} which was adjusted according to the onset of measured (or otherwise predicted; table 2) $4f^N \rightarrow 4f^{N-1}5d$ absorption. An explanation follows for the chosen parameter values.

Although the Hamiltonians for the $4f^N$ configuration and the $4f^{N-1}$ core of the $4f^{N-1}5d$ configuration both contain H(4f), the parameter values for these may be slightly different due to the contraction of 4f orbitals in the $4f^{N-1}5d$ configuration. The parameters of H(4f) for the $4f^N$ configuration were obtained from previous fittings of $4f^N$ levels, or by extrapolation from the same lanthanide ions in similar hosts. These parameters were already available for Ln = Ce [2], Eu, Gd [14], Er [15], Tm [16] and Yb [17]. The same parameters as for the $4f^N$ configuration were used for the $4f^{N-1}5d$ core, except for F^k ($k = 2, 4, 6$) and ζ_{4f}, which were enlarged from those values for the $4f^N$ configuration by the *ab initio* ratio 1.06 from [18]. The crystal-field parameter B_4(d) was available for Ln = Ce [2] and Pr [3] and was chosen to increase linearly throughout the series. The 5d electron spin–orbit coupling constant, ζ_{5d}, was calculated from experimental data for Ce^{3+} [2] and Tb^{3+} [4] and these values turned out to be 0.733 and 0.748 times the Hartree–Fock values [18], respectively. The values of ζ_{5d} were not available for the other Ln^{3+}, so the scaled Hartree–Fock values (by the factor 0.74) were employed. The parameters for the Coulomb interaction between the 4f and 5d electrons, F^k(fd) ($k = 2, 4$) and G^k(fd) ($k = 1, 3, 5$) from Hartree–Fock calculations are much too large and were scaled by the factor η_{fd} [11, 19]. The factor 0.53 was chosen throughout, as determined from the high spin–low spin $4f^7 5d$ separation in $Cs_2NaTbCl_6$ [4]. The other $4f^{N-1}$ parameters are relatively unimportant in our calculations, so the same values as for $4f^N$ were employed.

The transitions between the configurations $4f^N$ and $4f^{N-1}5d$ are electric dipole allowed and it is straightforward to calculate the matrix elements of the electric dipole moment operator connecting multi-electron wavefunctions of $4f^N$ and $4f^{N-1}5d$. The calculated locations and intensities of zero-phonon lines are displayed as sticks in the simulated spectra, on the left-hand side of the experimental results in figures 2–6. The metal–ligand interaction of 5d orbitals is different from (and much stronger than) that of 4f orbitals, so there is generally a displacement for the equilibrium positions of ligands during f–d transitions. Such a displacement results in the broad bands and consequently large Stokes shifts of vibronic structure of the absorption and emission spectra. The detailed vibronic structures are not well-resolved, so their crude simulation proposed by Reid *et al* [13] was adopted, i.e., by using Gaussian curves displaced towards higher energy from the zero-phonon lines by $E_{shift} = 600$ cm^{-1} and $E_{width} = 1000$ cm^{-1}, as estimated from the experimental spectra. These curves are displayed as full lines in the simulated spectra. The package written by Professor M F Reid was used to perform all the calculations.

Some additional spectral features have been observed in the excitation spectra of Cs_2NaYF_6:Ln^{3+} which are due to CT transitions and band-to-band transitions [9]. The measured and estimated lowest $4f^N - 4f^{N-1}5d$ absorption energy, E_{4f-5d}, and CT energy, E_{CT}, for the lanthanide ions in $Cs_2NaLnCl_6$ investigated are listed in table 2. The lowest 4f–5d energy E_{4f-5d} was predicted for spin-forbidden (in parentheses; table 2) and spin-allowed transitions using the phenomenological methods of Dorenbos [20, 21]:

$$E_{4f-5d}(\mathrm{Ln2, host}) = E_{4f-5d}(\mathrm{Ln1, host}) + \Delta E_{4f-5d}(\mathrm{Ln2, Ln1}), \quad (2)$$

and the CT energy was predicted using

$$E_{CT}(\mathrm{Ln2, host}) = E_{CT}(\mathrm{Ln1, host}) + \Delta E_{CT}(\mathrm{Ln2, Ln1}). \quad (3)$$

The values ΔE_{4f-5d} [20] and ΔE_{CT} [21] are given relative to Ce^{3+} and Eu^{3+}, which have the lowest 4f–5d and CT energy, respectively. Finally, the energies measured at ∼10 K for the *maxima* of the excitonic transitions near the conduction band edge are also listed in table 2, under CB.

4. Results and discussion

The emission and excitation spectra of neat and doped lanthanide hexachloroelpasolites are presented in figures 2–6.

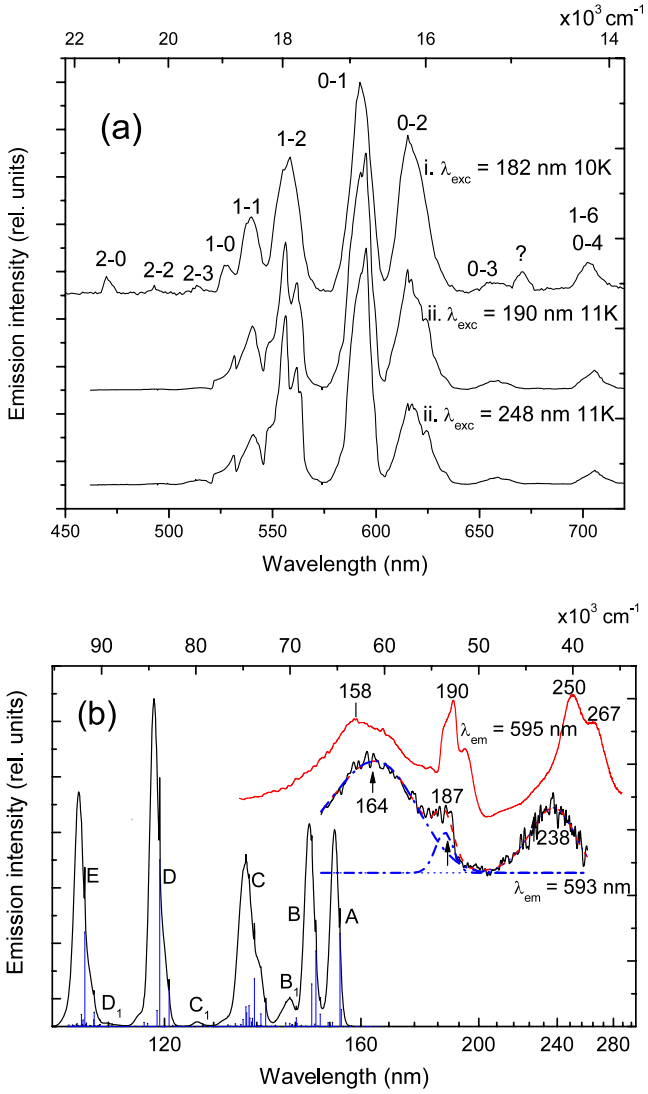

Figure 2. $Cs_2NaEuCl_6$. (a) Emission spectra of crystals (i) and (ii) between 450 and 720 nm at 10–11 K. The bands are identified with upper ^5D_J multiplet to lower ^7F_J transitions; see section 4.2. (b) Excitation spectra between 95 and 300 nm obtained by monitoring the 593 nm and 595 nm emission at 10 K (crystal (ii)) and 11 K (crystal (i)), respectively.

Note the linear and reciprocal lower wavelength scales for emission and excitation spectra, respectively.

4.1. $Cs_2NaYCl_6:Ce^{3+}$

The simplest 4f $\rightarrow$ 5d spectra occur for Ce^{3+}, which in octahedral symmetry has the lower t_{2g} orbital separated from e_g by 10 Dq = (10/21)B_4(d). The $(4f^1)^2F_{5/2}\Gamma_{7u} \rightarrow (5d^1)T_{2g}(\Gamma_{8g}, \Gamma_{7g})$ absorption spectra of $Cs_2NaYCl_6:Ce^{3+}$ have previously been reported, as well as the emission from the $T_{2g}(\Gamma_{8g})$ crystal-field level [2]. At low temperature, the emission transition to low energy of 28 193 cm^{-1} (354 nm) occurs. Emission from the upper $(5d^1)E_g\Gamma_{8g}$ level was also reported in [2] using 199.8 nm laser excitation.

Our present spectra of $Cs_2NaYCl_6:Ce^{3+}$ (0.1 at.%) obtained using synchrotron radiation gave at 11 K, under excitation at 210 nm, a broad emission band with FWHM of 183 nm, with a maximum at 472 nm and a shoulder at 374 nm. The first wavelength is similar to that for the sample of neat Cs_2NaYCl_6, whereas the shoulder is as expected from T_{2g} emission. The 11 K excitation spectrum of $Cs_2NaYCl_6:Ce^{3+}$ obtained by monitoring the 450 nm emission shows three bands at 35 984, 40 209 and 48 450 cm^{-1}, which are unassigned, in addition to the band-to-band transition at 55 617 cm^{-1} (180 nm). Broad emission bands were also previously reported for $Rb_2NaYF_6:Ce^{3+}$ [22] which were associated with Ce^{3+} at several sites, but their origin (as well as the broad emission bands observed herein) could otherwise be due to various Ce^{3+}–O^{2-} species, for which spectra have been presented elsewhere [23].

4.2. $Cs_2NaEuCl_6$

The emission of $Cs_2NaEuCl_6$ under 182 nm synchrotron radiation excitation was detected in the 200–1000 nm range at 10 K and only intraconfigurational $4f^6 - 4f^6$ transitions were observed. The electronic energy levels of Eu^{3+} in cubic elpasolites up to $^5D_3$ (24 329 cm^{-1}) and $^5F_2$ (about 33 520 cm^{-1}) have been characterized by means of conventional one-photon absorption and emission (see [14] and references therein) and two-photon absorption [24], respectively. Figure 2(a) shows the spectral range of the emission spectrum between 450 and 720 nm, using different excitation lines for two crystals, (i) and (ii). The peaks are marked according to the multiplet–multiplet transitions although in many cases the bands represent convoluted, unresolved vibronic and electronic transitions. Detailed assignments under higher resolution have been given elsewhere [25–27]. The highest energy emission from the neat elpasolite crystal (i) is from the $^5D_2$ multiplet, so possible higher luminescent levels are depopulated by nonradiative cross-relaxation processes. However, even this emission was quenched for crystal (ii), presumably due to oxide or hydroxide impurities.

The excitation spectra were recorded in the 150–300 nm range by monitoring the $^5D_0 \rightarrow {}^7F_1$ magnetic dipole emission from the two samples (i), (ii), as shown in figure 2(b). The calculated line strengths for f–d absorption as well as the simulated spectra are also included in the figure. The onset of f–d absorption is predicted to be at 64 100 cm^{-1} (156 nm), so the bands in the measured excitation spectra are not due to $4f^6 - 4f^5 5d^1$ transitions. The lower excitation spectrum (λ_{em} = 593 nm: crystal (ii)) was very noisy and has been smoothed and fitted with three Gaussian peaks centered at 164, 187 and 238 nm. The upper excitation spectrum from the other sample (λ_{em} = 595 nm: crystal (ii)) shows similar features except that the bands near 190 nm (shoulders at 195, 186 nm and maximum at 190 nm) are more prominent. The 190 nm band is assigned to the near excitonic band. Presumably the noisy spectrum was from a poorer quality crystal, so surface losses were much greater and the band-to-band excitation resulted in transfer to nonradiative trap sites rather than to Eu^{3+} levels.

The CT energy of Eu^{3+} in crystals is the lowest out of all the Ln^{3+} series and is measured at 267 nm for $Cs_2NaEuCl_6$,

which is comparable with the location (301 nm; 33 200 cm^{-1}) of the charge transfer band of $EuCl_3{\cdot}xH_2O$ dissolved in a saturated solution of $(C_2H_5)_4NCl$ in acetonitrile [6]. The bands at 238 nm (crystal (ii)) and 250 nm (crystal (i)) are too high in energy to be assigned to the Cl^-–Eu^{3+} CT in $Cs_2NaEuCl_6$. Since the sample was exposed to air it contains some oxygen-species impurities. The CT absorption from O^{2-} impurities in YF_3 to Eu^{3+} has been observed to be 42 100 cm^{-1} (238 nm) [28], and at 230–250 nm in Y_2O_3 [29], which prompts us to assign the band in this region in the excitation spectra of figure 2(b) to O^{2-} to Eu^{3+} CT transition.

This leaves the band at 158–164 nm unassigned. One possible explanation for this band is the CT transition to the excited $4f^65d^1$ configuration of Eu^{2+}, although Ionova *et al* [7] calculate rather a higher energy (∼95 000 cm^{-1}; 105 nm) for this transition. The estimation of the separation between the lowest energy level of $4f^65d^1$ and the ground state, $4f^7Eu^{2+}$, is about 25 000 cm^{-1} for Cl^- ligands, from $SrCl_2$:Eu^{2+} [30]. The estimated energy for the excitation of an electron from the valence band to an empty 5d orbital of Eu^{2+} is therefore 37 310 + 25 000 cm^{-1} = 62 310 cm^{-1} (∼161 nm).

4.3. $Cs_2NaGdCl_6$

The emission of $Cs_2NaGdCl_6$ under 185 nm synchrotron radiation excitation was detected in the 300–550 nm range at 11 K (figure 3(a)). The spectrum shows, apart from the well-known $^6P_{7/2}$ emission at ∼31 500 cm^{-1} [31], some other structured emission bands in the range 380–540 nm which are assigned to $^5D_3 \rightarrow {}^7F_J$ (J = 6–2) and $^5D_4 \rightarrow {}^7F_6$ transitions of inadvertently introduced Tb^{3+} impurity [32].

The stable half-filled $4f^7$ configuration makes both the energy of the lowest 5d levels (predicted herein to be at ∼74 000 cm^{-1}) and the energy of the CT band (∼70 000 cm^{-1} [7]) very high. The excitation spectrum obtained by monitoring the 312 nm $^6P_{7/2} \rightarrow {}^8S_{7/2}$ emission at 11 K (figure 3(b)) contains both very sharp peaks (for $4f^7$ – $4f^7$ absorption bands) and some broad features. The band with a maximum at 183 nm and a shoulder at 189 nm is related to conduction band absorption. The structure to high energy of this band bears some resemblance, though at different energies, to the excitation spectra of some other hexachloroelpasolites. It may therefore be due to absorptions associated with the host and a density of states calculation would be useful. The broader structure at 219 nm and at ∼240 nm, where it underlies sharp $4f^7$ – $4f^7$ transitions, is not due to Tb^{3+} and is probably due to an oxygen-species impurity. In fact, the room temperature synchrotron radiation excitation spectrum of $Cs_2NaGdCl_6$ has previously been reported by Dereń *et al* [33] and there were no features observed to higher energy of the intense band at ∼240 nm. Many of the energy levels of $Cs_2NaGdCl_6$ between 31 954 and 40 721 cm^{-1} have been determined by two-photon spectroscopy [34]. The weak, lowest energy feature in figure 3(b) at 280.6 nm (35 634 cm^{-1}) corresponds to the $^8S_{7/2} \rightarrow {}^6I_{7/2}\Gamma_7$ zero-phonon line. The spectral resolution is however insufficient for resolving individual vibronic origins, so a detailed interpretation of the $4f^7$ – $4f^7$ excitation spectrum from figure 3(b) is not possible. It

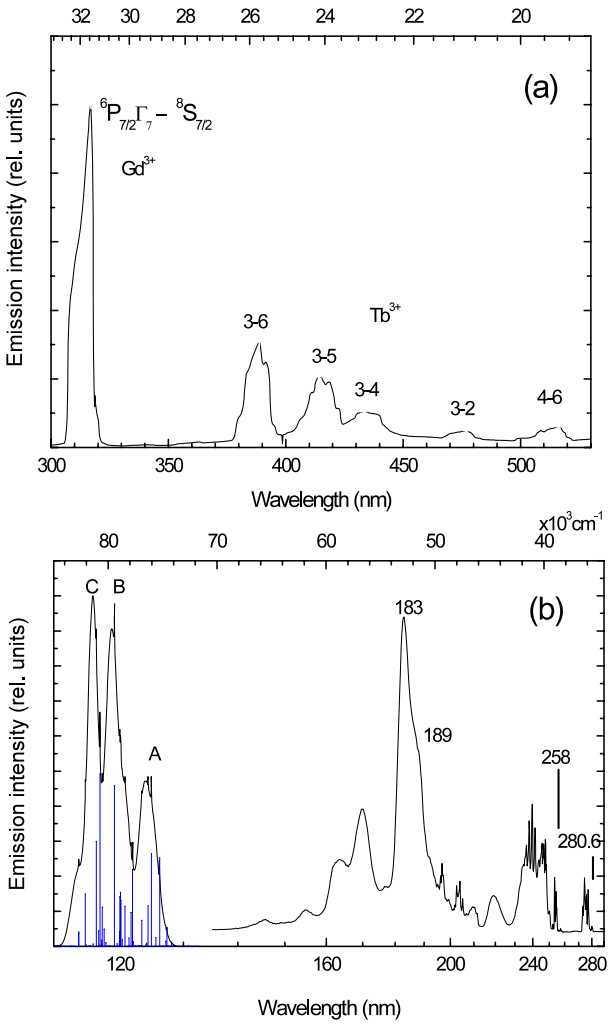

Figure 3. $Cs_2NaGdCl_6$. (a) 185 nm emission spectrum between 285 and 530 nm at 11 K. The Tb^{3+} transitions correspond to unresolved $^5D_J \rightarrow {}^7F_J$ structures, as numbered. (b) 11 K excitation spectrum obtained by monitoring the 312 nm emission.

is noted that there is an energy gap of 2712 cm^{-1} in the tabulation of [34] between the levels $^6I_{15/2}\Gamma_6$ (36 507 cm^{-1}) and $^6D_{5/2}\Gamma_6$ (39 219 cm^{-1}). Infrared luminescence would therefore be expected from $^6D_{5/2}$ in this host lattice. Also, the spectrum of figure 3(b) shows features commencing at the rather longer wavelength of 258 nm (38 788 cm^{-1}) for the $^6D_{5/2}$ group, which cannot correspond to hot electronic or vibronic structure, so a high resolution absorption spectrum in this region would be of interest.

4.4. $Cs_2NaErCl_6$

The elpasolite $Cs_2NaErCl_6$ has many luminescent levels spanning the ultraviolet to infrared spectral regions and the energy levels have been well-documented [15]. Also, with the use of synchrotron radiation, the room temperature emission and excitation spectra of $Cs_2NaErCl_6$ have been presented [35]. These results showed that the highest luminescent level is the $^2I_{11/2}$ multiplet (∼40 600 cm^{-1}) and that many ion–ion cross-relaxation processes occur in the neat material. From the 300 K

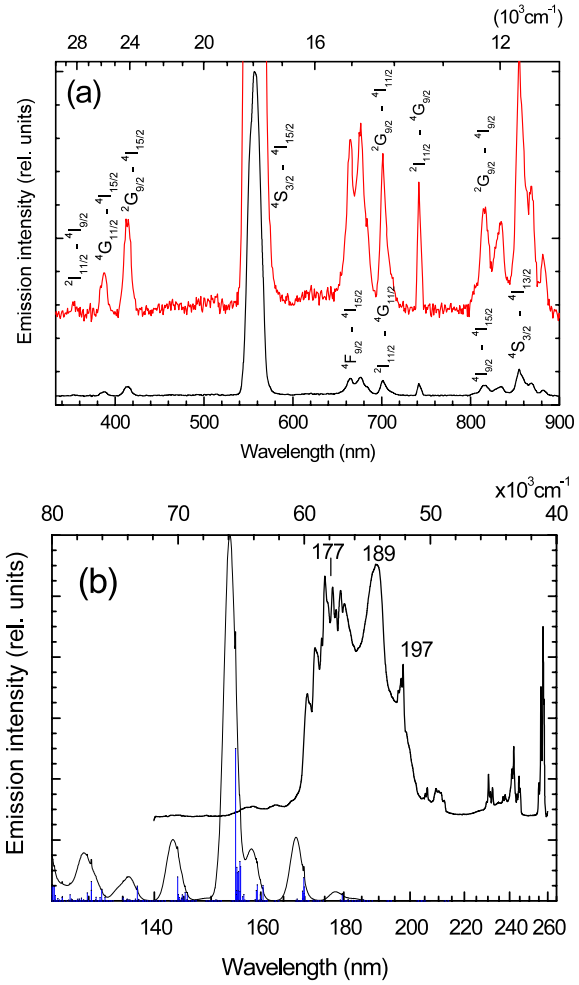

Figure 4. $Cs_2NaErCl_6$. (a) 10 K emission spectrum obtained using 182 nm excitation. (b) 11 K excitation spectrum between 140 and 260 nm obtained by monitoring the 545 nm emission.

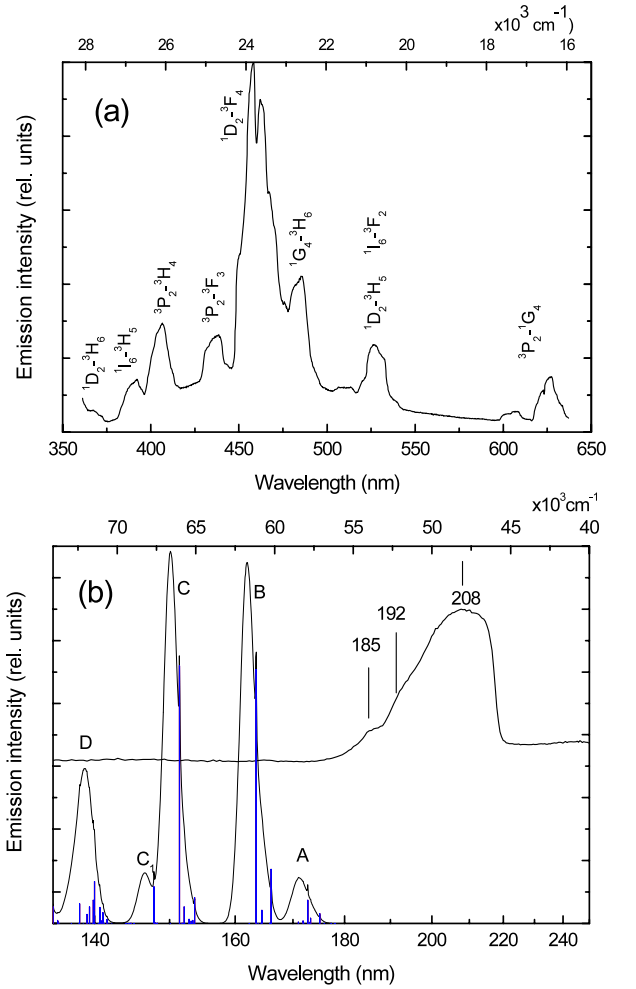

Figure 5. Cs_2NaYCl_6:Tm^{3+}. (a) 200 nm excited emission spectrum between 350 and 650 nm at 11 K. (b) 11 K excitation spectrum of the 460 nm emission between 130 and 245 nm.

excitation spectra, the charge transfer band was assigned at 182 nm and the absorption from the valence band to the near edge of the conduction band was around 197–201 nm.

The low temperature emission spectrum under 182 nm synchrotron radiation excitation is presented in figure 4(a), and the excitation spectrum obtained by monitoring the $^4S_{3/2} \rightarrow {}^4I_{15/2}$ emission is in figure 4(b). The $^4S_{3/2} \rightarrow {}^4I_{15/2}$ emission dominates figure 4(a), which indicates that the absorption state(s) finally relax(es) mostly to $^4S_{3/2}$, due to various nonradiative decay and cross-relaxation processes. Weaker emission transitions are observed from $^2I_{11/2}$, $^4G_{11/2}$, $^2G_{9/2}$, $^4F_{9/2}$, and $^4I_{9/2}$ multiplets, as indicated in the figure. The excitation spectrum is more difficult to assign and a tentative explanation is given here. A shoulder is observed at 197 nm (50 760 cm^{-1}) and it is decorated with $4f^{11} \rightarrow 4f^{11}$ absorption bands. The strong band to higher energy at 189 nm (52 880 cm^{-1}) is related to the band-to-band transition. The CT absorption corresponds to the broad band to high energy (∼177 nm) which is decorated with fine structure, and may be coincident with the host band structure. The reappearance of this fine structure is different from the reappearance of fine structure in the excitation spectra of Tb^{3+}, Er^{3+} and Tm^{3+} in CaF_2 and $LiYF_4$, where the d electron changes occupation from an e_g to a t_{2g} orbital [36]. In this case, the fine structure is due either to $4f^{11} \rightarrow 4f^{11}$ transitions or to spin-forbidden $4f^{11} \rightarrow 4f^{10}5d^1$ transitions. The onsets of spin-forbidden and spin-allowed $4f^{11} \rightarrow 4f^{10}5d^1$ absorptions are predicted to be at 55 150 cm^{-1} (181 nm) and 58 200 cm^{-1} (172 nm), so the 4f–5d absorption is calculated to become much stronger towards higher energy.

4.5. Cs_2NaYCl_6:Tm^{3+}

The emission spectrum was measured under 200 nm synchrotron radiation excitation at 11 K and is shown in figure 5(a). Luminescence from $^3P_2$ (37 460 cm^{-1}) [37], $^1I_6$ (34 117 cm^{-1}), $^1D_2$ (27 653 cm^{-1}) and $^1G_4$ (20 852 cm^{-1}) [16] has been reported previously under high resolution at low temperature for $TmCl_6^{3-}$. In addition, luminescence is clearly assigned in figure 5(a) from $^1I_6$, and the features with maxima at 25 499 cm^{-1} (392 nm) and 18 995 cm^{-1} (526 nm) correspond to the transitions to terminal $^3H_5$ and $^3F_2$ multiplets.

The energy of CT absorption was calculated by Ionova *et al* [7] to be close to 210 nm (48 000 cm^{-1}), which is lower than the value estimated using the method provided by Dorenbos [21], which is at 193 nm (51 800 cm^{-1}), using the CT value for Eu^{3+} (267 nm). This difference is acceptable in view of the broad-band nature of CT bands and the allowed deviations of the phenomenological method.

The 11 K excitation spectrum of the 460 nm emission is shown in figure 5(b). It contains a broad band centered at 208 nm with shoulders on the high energy side, at 185 and 192 nm. Since the inter-band absorption is expected to change only slightly for the series of crystals $Cs_2NaLnCl_6$ (Ln = Y, Eu, Gd, Er, Tm and Yb), the shoulders may be assigned to the inter-band absorption and the 208 nm band to CT absorption. The calculated $4f^{12} \rightarrow 4f^{11}5d$ transitions are also shown in figure 5(b). The onsets of spin-forbidden and spin-allowed f–d absorptions are predicted at 55 150 cm^{-1} (181 nm) and 57 200 cm^{-1} (175 nm), respectively, and are not observed in the excitation spectrum. A very weak, broad band (not shown in the excitation spectrum of figure 5(b)) is observed at 246 nm.

4.6. $Cs_2NaYbCl_6$

The emission spectrum of $Cs_2NaYbCl_6$ was recorded in the range 300–600 nm in order to detect possible CT emission under the 175 nm synchrotron radiation excitation. The emission signal was very weak and the spectrum, figure 6(a), turned out to be almost the same as that of Cs_2NaYCl_6:Tm^{3+}, but shifted by 4.58 nm to lower energy. This shows that the emission is actually due to Tm^{3+} impurity in $Cs_2NaYbCl_6$.

The excitation spectrum for the strongest emission at 460 nm was detected in the range of 120–220 nm (figure 6(b)). The spectrum shows a sharp structure between 170 and 180 nm and a weak and broad band at 208 nm. The sharp structure is presumably due to fluctuation of the weak signal of emission and hence may be an artifact, and the band at 208 nm is the CT band of Tm^{3+} impurities. It is interesting that the relative intensities of these two bands are the reverse of the corresponding features in figure 5(b), because the CT intensity is proportional to the concentration of Tm^{3+} in the crystal.

The onset of $4f^{13} \rightarrow 4f^{12}5d$ absorption is predicted to be at 151 nm (66 200 cm^{-1}) and is not observed in the excitation spectrum. Also, the CT absorption is predicted to be at 245 nm (40 800 cm^{-1}) and is not within the range of detection.

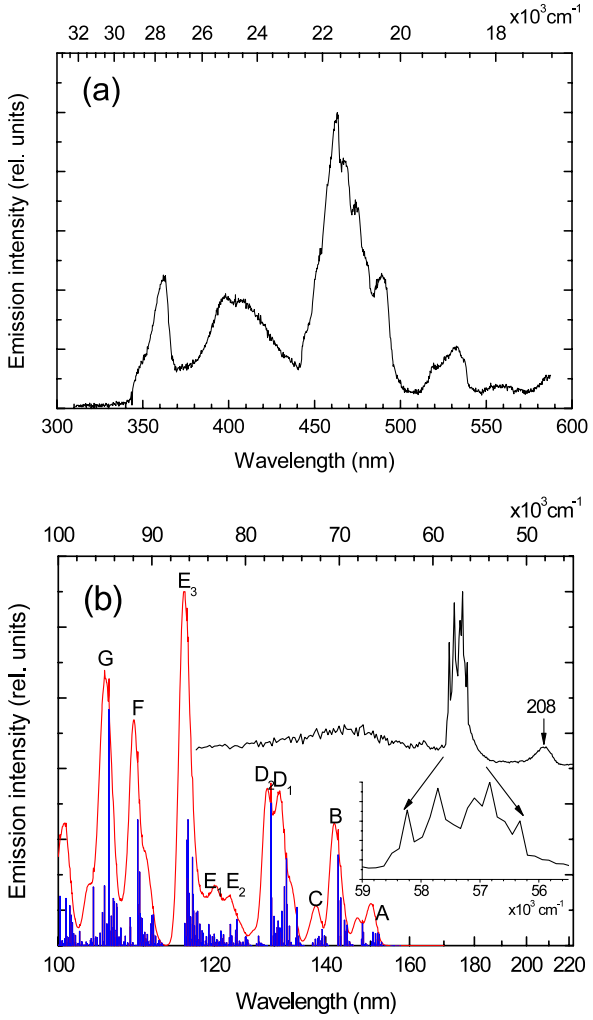

Figure 6. $Cs_2NaYbCl_6$. (a) 175 nm excited emission spectrum at 11 K. The bands correspond to Tm^{3+} trace impurity. (b) 11 K excitation spectrum between 120 and 230 nm obtained by monitoring the 460 nm emission.

5. Conclusions

The results herein provide a stark contrast to the analogous ones for the hexafluoroelpasolites Cs_2NaYF_6:Ln^{3+} (Ln = Nd, Ho, Tm, Yb) [9] where (with the exception of the Yb^{3+} case) the f–d excitation transitions of Ln^{3+} were observed below the host band gaps. In addition, interconfigurational d–f emission transitions were reported for several hexafluoroelpasolite systems: Nd^{3+} [38] Er^{3+} and Tm^{3+} [39]. For the hexachloroelpasolites, $Cs_2NaLnCl_6$, although interconfigurational f–d absorption transitions have previously been reported for several Ln^{3+} cases, as mentioned in the Introduction, f–d excitation or d–f emission transitions have not been observed for the ions studied herein. Instead, the synchrotron excitation spectra comprised 4f–4f transitions, CT transitions, and various bands due to impurities. A feature occurring in most of the excitation spectra is a strong band near 190 nm which has been associated with an excitonic transition near the band edge.

The simulated f–d absorption spectra have been presented, from calculations which did not require the fitting of parameters, but rather where parameters were allocated previously assigned values from the literature, or where extrapolations were performed.

Acknowledgments

Financial support for this work from the Hong Kong Research grants Council General Research Fund Grant CityU 102308 is gratefully acknowledged. This work was also supported by the National Science Foundation of China, under Grant No. 10874253.

References

[1] Tanner P A 2004 *Top. Curr. Chem.* **241** 167
[2] Tanner P A, Mak C S K, Edelstein N M, Liu G, Huang J, Seijo L and Barandiaran Z 2003 *J. Am. Chem. Soc.* **125** 13225
[3] Tanner P A, Mak C S K, Faucher M D, Kwok W M, Phillips D L and Mikhailik V 2003 *Phys. Rev.* B **67** 115102
[4] Ning L, Mak C S K and Tanner P A 2005 *Phys. Rev.* B **72** 085127
[5] Collombet A, Guyot Y, Mak C S K, Tanner P A and Joubert M-F 2001 *J. Lumin.* **94** 39
[6] Ryan J L and Jørgensen C K 1966 *J. Phys. Chem.* **70** 2845
[7] Ionova G, Krupa J C, Gérard I and Guillaumont R 1995 *New J. Chem.* **19** 677
[8] Makhov V N, Khaidukov N M, Lo D, Krupa J C, Kirm M and Negodin E 2005 *Opt. Mater.* **27** 1131
[9] Duan C–K, Tanner P A, Babin V and Meijerink A 2009 *J. Phys. Chem.* C **113** 12580
[10] van Pieterson L, Reid M F, Wegh R T, Soverna S and Meijerink A 2002 *Phys. Rev.* B **65** 045113
[11] van Pieterson L, Reid M F, Burdick G W and Meijerink A 2002 *Phys. Rev.* B **65** 045114
[12] Wegh R T and Meijerink A 1999 *Phys. Rev.* B **60** 10820
[13] Reid M F, van Pieterson L, Wegh R T and Meijerink A 2000 *Phys. Rev.* B **62** 14744
[14] Tanner P A, Kumar V V R K, Jayasankar C K and Reid M F 1994 *J. Alloys Compounds* **215** 349
[15] Faucher M D and Tanner P A 2003 *Mol. Phys.* **101** 983
[16] Faucher M D, Tanner P A and Mak C S K 2004 *J. Phys. Chem.* A **108** 5278
[17] Zhou X, Reid M F, Faucher M D and Tanner P A 2006 *J. Phys. Chem.* B **110** 14939
[18] Reid M F, van Pieterson L and Meijerink A 2001 *J. Alloys Compounds* **344** 240
[19] van Pieterson L, Reid M F, Burdick G W and Meijerink A 2002 *Phys. Rev.* B **65** 045113
[20] Dorenbos P 2000 *J. Lumin.* **91** 155
[21] Dorenbos P 2009 *J. Alloys Compounds* at press doi:10.1016/j.jallcom.2008.09.059
[22] Aull B and Jenssen H P 1986 *Phys. Rev.* B **34** 6647
[23] Kodama N, Yamaga M and Henderson B 1998 *J. Appl. Phys.* **84** 5820
[24] Thorne J R G, Jones M, McCaw C S, Murdoch K M, Denning R G and Khaidukov N M 1999 *J. Phys.: Condens. Matter* **11** 7851
[25] Serra O A and Thompson L C 1976 *Inorg. Chem.* **15** 504
[26] Morley J P, Faulkner T R and Richardson F S 1982 *J. Chem. Phys.* **77** 1710
[27] Flint C D and Stewart-Darling F L 1981 *Mol. Phys.* **44** 61
[28] Belsky A N and Krupa J C 1999 *Displays* **19** 185
[29] Tanner P A, Fu L and Cheng B-M 2009 *J. Phys. Chem.* C **113** 10773
[30] Pan Z, Ning L, Cheng B-M and Tanner P A 2006 *Chem. Phys. Lett.* **428** 78
[31] de Vries A J and Blasse G 1988 *J. Chem. Phys.* **88** 7312
[32] Thompson L C, Serra O A, Riehl J P, Richardson F S and Schwartz R W 1977 *Chem. Phys.* **26** 393
[33] Dereń P J, Strek W and Krupa J-C 1998 *Chem. Phys. Lett.* **298** 217
[34] Kundu L, Banerjee A K and Chowdhury M 1991 *Chem. Phys. Lett.* **181** 569
[35] Zhou X, Tanner P A, Duan C K and Cheng B-M 2007 *Chem. Phys. Lett.* **442** 302
[36] van Pieterson L, Reid M F and Meijerink A 2002 *Phys. Rev. Lett.* **88** 067405
[37] Tanner P A, Mak C S K, Kwok W M, Phillips D L and Joubert M F 2002 *J. Phys. Chem.* B **106** 3606
[38] Tanner P A, Ning L, Makhov V N, Khaidukov N M and Kirm M 2006 *J. Phys. Chem.* B **110** 12113
[39] Makhov V N, Khaidukov N M, Lo D, Krupa J C, Kirm M and Negodin E 2005 *Opt. Mater.* **27** 1131